CHEMBIOCHEM

DOI: 10.1002/cbic.200800467

# Hydrogen-Bond Detection, Configuration Assignment and Rotamer Correction of Side-Chain Amides in Large Proteins by NMR Spectroscopy through Protium/Deuterium Isotope Effects

Aizhuo Liu,*[a] Jifeng Wang,[a] Zhenwei Lu,[a] Lishan Yao,[a, b] Yue Li,[a] and Honggao Yan*[a]

*The configuration and hydrogen-bonding network of side-chain amides in a 35 kDa protein were determined by measuring differential and trans-hydrogen-bond H/D isotope effects by using the isotopomer-selective (IS)-TROSY technique, which leads to a reliable recognition and correction of erroneous rotamers that are frequently found in protein structures. First, the differential two-bond isotope effects on carbonyl $^{13}C'$ shifts, which are defined as $\Delta^2\Delta^{13}C'(ND) = {}^2\Delta^{13}C'(ND^E) - {}^2\Delta^{13}C'(ND^Z)$, provide a reliable means for the configuration assignment for side-chain amides, because environmental effects (hydrogen bonds and charges, etc.) are greatly attenuated over the two bonds that separate the carbon and hydrogen atoms, and the isotope effects fall into a narrow range of positive values. Second and more importantly, the significant variations in the differential one-bond isotope effects on $^{15}N$ chemical shifts, which are defined as $\Delta^1\Delta^{15}N(D) = {}^1\Delta^{15}N(D^E) - {}^1\Delta^{15}N(D^Z)$ can be correlated with hydrogen-bonding interactions, particularly those involving charged acceptors. The differential one-bond isotope effects are additive, with major contributions from intrinsic differential conjugative interactions between the* E *and* Z *configurations, H-bonding interactions, and charge effects. Furthermore, the pattern of trans-H-bond H/D isotope effects can be mapped onto more complicated hydrogen-bonding networks that involve bifurcated hydrogen-bonds. Third, the correlations between $\Delta^1\Delta^{15}N(D)$ and hydrogen-bonding interactions afford an effective means for the correction of erroneous rotamer assignments of side-chain amides. Rotamer correction by differential isotope effects is not only robust, but also simple and can be applied to large proteins.*

## Introduction

The carboxamide moieties of asparagine and glutamine residues in proteins can serve as hydrogen-bond (H-bond) donors, acceptors, or both, and are frequently involved in H-bond networks. Consequently, Asn and Gln residues are often found in the active centers of enzymes and critical elements of other proteins, and play important roles in molecular recognition, catalysis, structure, and stability.[1]

Despite their chemical and biological importance, H bonds are least-well defined in protein structures, which are mainly determined by X-ray crystallography and NMR spectroscopy. In general, X-ray cannot "see" hydrogen atoms in most protein crystals, and the positions of hydrogen atoms are consequently not defined. On the other hand, NMR structure calculations rely on mostly the distances between hydrogen atoms and the positions of the heavy atoms involved in hydrogen bonds are defined by standard covalent geometry information. In the case of side-chain carboxamides, the identities of the nitrogen and oxygen atoms are also hard to recognize by X-ray crystallography because the nitrogen and oxygen atoms within a carboxamide group are related by a twofold symmetrical axis and their electron density maps are very similar. Consequently, erroneous rotamer assignments of side-chain amides are frequently found in protein crystal structures. It has been estimated[2] that ~20% of side-chain amide rotamers are incorrect in protein crystal structures deposited in the Protein Data Bank (PDB).[3] A similar error rate in solution NMR spectroscopic structures of proteins has also been estimated.[4]

One of the most important advances in NMR spectroscopy in the last decade was the *direct* detection of H bonds through trans-hydrogen-bond scalar couplings. Trans-hydrogen-bond scalar couplings are generally small and thus cannot be measured for large proteins. Unlike the electron-mediating scalar couplings, isotope effects are intrinsically vibrational phenomena; however, because isotope effects can be transmitted through covalent bonds as well as H bonds, potentially they can be used as an alternative means for the *direct* detection of H bonds.

The usefulness of isotope effects in NMR analysis of compounds, small proteins, and nucleic acids has been widely

[a] Prof. Dr. A. Liu, J. Wang, Z. Lu, Dr. L. Yao, Dr. Y. Li, Prof. Dr. H. Yan
Department of Biochemistry and Molecular Biology
Michigan State University
East Lansing, MI 48824 (USA)
Fax: (+1) 517-353-9334
E-mail: liua@msu.edu
yanh@msu.edu

[b] Dr. L. Yao
Present address: Laboratory of Chemical Physics
NIDDK, National Institute of Health
Bethesda, MD 20892 (USA)

Supporting information for this article is available on the WWW under http://www.chembiochem.org or from the author.

reported in the literature.[5–6] Several lines of evidence have shown a clear correlation between primary deuterium (D) isotope effects and the strength of H bonds.[7–8] Because the NMR spectroscopic direct observation of deuterium is limited by the experimental conditions, broad linewidth, and low sensitivity, current studies have been focused on secondary H/D isotope effects. With the advent of triple-resonance NMR spectroscopic techniques and the availability of isotope-enriched materials, extensive and in-depth studies on deuterium isotope effects on the chemical shifts of proteins and nucleic acids have become possible. For instance, the 2D HA(CA)CO experiment has been used for measuring $^{2}\Delta^{13}C'(ND)$ in the study of the equilibrium protium/deuterium fractionation of backbone amides in human ubiquitin;[9] $^{3}\Delta^{13}C^{\alpha}(ND)$ and $^{2}\Delta^{13}C^{\alpha}(ND)$ isotope effects have been measured with 3D HCA(CO)N and 3D HCAN experiments, respectively, for the correlation of $^{13}C^{\alpha}$ chemical shifts with the backbone conformation;[10] backbone $^{2}\Delta^{13}C'(ND)$, $^{3}\Delta^{13}C^{\alpha}(ND)$ and $^{3}\Delta^{13}C^{\beta}(ND)$ isotope effects have also been measured with new editing and filtering techniques.[11–12] Because isotope effects on chemical shifts are generally small, most of their biological applications to date have been limited to small proteins and nucleic acids. Deuterium isotope effects on protein side-chain amides have rarely been studied because side-chain amide resonances are normally invisible in standard TROSY-based NMR spectroscopy experiments, which are required for large proteins. Recently, we have demonstrated that the TROSY methodology can be adapted for the detection of the NMR spectroscopic signals of side-chain amides with a significantly enhanced sensitivity, particularly for large proteins, through the combined use of a 1:1 $H_2O/D_2O$ solvent mixture and deuterium decoupling.[13–14] The new TROSY technique, dubbed isotopomer-selective (IS)-TROSY, exclusively detects semideuterated isotopomers of carboxamide groups of Asn/Gln residues in large proteins with high sensitivities just as the detection of backbone amides with standard TROSY experiments.

The two primary amide protons within a side-chain carboxamide group usually show different chemical shifts, due to the slow interconverting rate that stems from the partial double-bond character of the C′-$N^{\delta/\varepsilon}$ (Asn/Gln) amide bonds. One of the geminal amide protons is in the *trans E* configuration with respect to the carboxamide oxygen and normally has a downfield (high frequency) chemical shift; the other, in the *cis Z* configuration, shows an upfield chemical shift. The order of their chemical shifts could be reversed, however, due to aromatic ring current effects and/or strong H-bonding interactions. Therefore, the stereospecific resonance assignment of side-chain amide protons is a prerequisite for further NMR spectroscopic studies of side-chain amides in proteins.

We report here the differential secondary H/D isotope effects on the side-chain amides of yeast cytosine deaminase (yCD), a 35 kDa homodimeric protein that was measured by the IS-TROSY-based technique. We show that the measurement of differential isotope effects is an effective means for the assignment of configurations, identification of hydrogen bonds, and correction of erroneous rotamers of side-chain amides.

## Results and Discussion

### Differential one-bond H/D isotope effects on side-chain carboxamide $^{15}N$ chemical shift

Although the understanding of isotope effects on NMR chemical shifts is incomplete, from accumulated experimental observations over decades, it is generally accepted that the magnitude of the isotope effects depends not only on the ratio of isotope masses but also on the chemical-shift range of the nucleus.[5,15] The larger the chemical-shift range of the nucleus, the larger are the isotope effects. For instance, the size of one-bond deuterium isotope effects on the chemical shift of amide $^{15}N$, defined as $^{1}\Delta^{15}N(D) = \delta^{15}N\{H\} - \delta^{15}N\{D\}$, is up to ~700 ppb in proteins, because amide $^{15}N$ chemical shifts are well dispersed. In protein backbones, variations in $^{1}\Delta^{15}N(D)$ depend primarily on the difference in hydrogen-bonding interactions[9] and electric field effects from charges in the vicinity of amide protons.[16–18] The effects of conformation are relatively small because the amide proton is typically in the *trans* configuration with respect to the carbonyl oxygen of the preceding residue.

For the side-chain carboxamides of Asn and Gln residues, the two geminal protons have different configurations. The N–$H^{E}$ bond is *trans* to the C=O bond and has a stretching frequency higher than that of the N–$H^{Z}$ bond, which is *cis* to the C=O bond. One of the important properties of amides is their tendency to involve the nitrogen atom lone pair in the carbonyl $\pi$ system; this results in the partial double-bond character, that is, both the C′–N and C′–O bonds have a bond order of 1.5, which makes the amide group planar and rigid. Consequently, the two geminal N–$H^{E}$ and N–$H^{Z}$ bonds have different orientations with respect to the adjacent $\pi$ orbitals, which is somewhat reminiscent of the much less restricted orientations of the two geminal C–$H^{\alpha}$ bonds in a glycine residue.[19] As a result of different (hyper)conjugations, the N–$H^{E}$ bond length is likely 1–2% shorter than that of the N–$H^{Z}$ bond as determined by neutron diffraction,[20–21] although the difference was not detected by solid state NMR spectroscopic measurements.[22] The configuration-dependent changes in the vibrational manifold lead to differential isotope effects, and it follows that $^{1}\Delta^{15}N(D^{E})$ is intrinsically larger than $^{1}\Delta^{15}N(D^{Z})$. In other words, the difference in the secondary isotope effects or the differential one-bond isotope effects, $\Delta^{1}\Delta^{15}N(D) = {}^{1}\Delta^{15}N(D^{E}) - {}^{1}\Delta^{15}N(D^{Z})$, is normally positive.

The measurement of one-bond H/D isotope effects, $^{1}\Delta^{15}N(D^{E/Z})$, is straightforward for small proteins, as illustrated in the top panel of Figure 1. In a standard $^{15}N,^{1}H$ HSQC spectrum recorded for a small protein in the $H_2O/D_2O$ solvent mixture, normally four resonances (dashed circles) for each side-chain amide can be observed, one pair from the fully protonated isotopomer (large dashed circles) at the downfield in the $^{15}N$ dimension and the other from the two semideuterated isotopomers (small dashed circles) at upfield. The neat differential H/D isotope effects on one-bond $^{15}N$ chemical shifts, $\Delta^{1}\Delta^{15}N(D)$, can, in principle, be measured from the $^{15}N$ chemical shift difference between the two semideuterated peaks

  

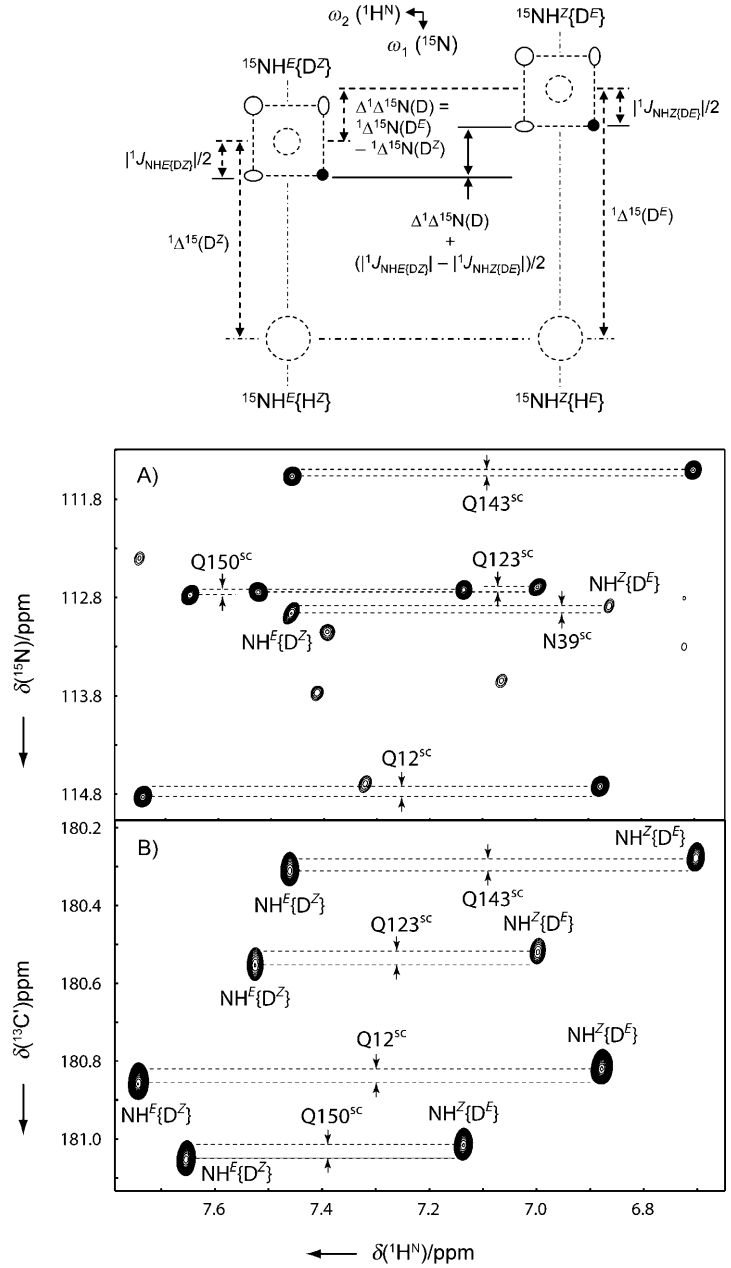


**Figure 1.** Regions of A) 2D $^{15}$N,$^1$H IS-TROSY and B) 2D IS-TROSY-H(N)CO spectra of yCD showing Asn/Gln side-chain amide resonance correlations. Above A) is a schematic diagram that illustrates how the differential H/D isotope effects on one-bond $^{15}$N chemical shifts, $\Delta^1\Delta^{15}N(D) = {}^1\Delta^{15}N(D^E) - {}^1\Delta^{15}N(D^Z)$, are measured in the 2D $^{15}$N,$^1$H IS-TROSY spectrum. Both spectra A) and B) were recorded by using a Bruker Avance 900 MHz NMR spectrometer that was equipped with a TCI cryoprobe at 25 °C with a u-$^2$H/$^{13}$C/$^{15}$N-labeled protein sample in 1:1 $H_2O/D_2O$. The differential H/D isotope effects on one-bond $^{15}$N chemical shifts, $\Delta^1\Delta^{15}N(D) = {}^1\Delta^{15}N(D^E) - {}^1\Delta^{15}N(D^Z)$, modified by scalar couplings, and on two-bond $^{13}$C′ chemical shifts, $\Delta^2\Delta^{13}C'(ND) = {}^2\Delta^{13}C'(ND^E) - {}^2\Delta^{13}C'(ND^Z)$, where *E* stands for the *trans* and *Z* the *cis* side-chain amide hydrogen atoms, can be accurately measured from the chemical-shift difference in the indirect dimension for the same carboxyamide moiety. Paired side-chain NH{D} resonances of each Asn/Gln residue are linked by two dash lines across the center of each resonance, and the chemical-shift difference is indicated with paired arrows. Stereospecific distinction between the *E* and *Z* protons can be achieved based on the difference in isotope effects (refer to the text for details). Spectrum A) was recorded with eight scans and a 2 s delay time, $t_{1max}(^{15}N) = 93$ ms and $t_{2max}(^1H^N) = 285$ ms; this resulted in the experimental time of 2.4 h; B) was recorded with 64 scans and a 1.8 s delay time, $t_{1max}(^{13}C) = 110$ ms and $t_{2max}(^1H^N) = 285$ ms; this resulted in the experimental time of 29.8 h. Before Fourier transformation, the raw data were zero-filled; this resulted in a 0.5 Hz digital resolution in the indirect dimension for spectrum A) and 1.0 Hz for B).

(the two smaller dashed circles) if there is no signal overlap and the sensitivity is high enough. For large proteins, however, the direct measurement of $^1\Delta^{15}$N(D) is often impossible because resonances of $^{15}NH_2$ isotopomers are weak due to the strong dipole–dipole interaction between the geminal protons, especially in the presence of H bonds,[13–14] and the chance of signal overlap is high. In the 2D $^{15}$N,$^1$H IS-TROSY spectrum, however, the two protonated resonances are filtered out,[23] and thus the spectrum is simplified. More importantly, the experiment exclusively detects the so-called TROSY peak with a high sensitivity, which is the lower right component of each quartet (the TROSY component is represented as a small filled circle, and the three non-TROSY components are as open circles).[13–14] Figure 1 A is a region of the 2D $^{15}$N,$^1$H IS-TROSY spectrum of yCD. The resonance of the $^{15}$N–H$^E${D$^Z$} isotopomer has the $^{15}$N chemical shift modified by the $^1\Delta^{15}N(D^Z)$ isotope effect from the *Z* position and that of the $^{15}$N–H$^Z${D$^E$} isotopomer by $^1\Delta^{15}N(D^E)$ from the *E* position. The measured differential one-bond isotope effects, $\Delta^1\Delta^{15}N(D) = {}^1\Delta^{15}N(D^E) - {}^1\Delta^{15}N(D^Z)$, are summarized in Table 1. Duplicated experiments indicate that the differential isotope effects could be measured with high accuracy (the standard error was less than 5 ppb). These differential isotope effects can be accurately measured even when the linewidth is larger than the chemical shift difference in the $^{15}$N dimension because the corresponding proton resonances are well separated, which is similar to the accurate measurement of small *J* couplings in exclusive correlation spectroscopy (E.COSY) type of spectra.[24] The adoption of the TROSY technique and deuteration actually makes the linewidth very narrow, even for large proteins.

As expected, most (ten out of eleven) of the $\Delta^1\Delta^{15}N(D)$ values for yCD were positive, which is characteristic of configurational effects, but their magnitudes varied significantly and one of them (Asn51) was even negative. The large variations in $\Delta^1\Delta^{15}N(D)$ indicate that the magnitude of $^1\Delta^{15}N(D)$ is sensitive to the H-bonding interactions that are involved, and to charges in the vicinity of the amide proton, which will be discussed later.

It is noteworthy that the apparent magnitude of $\Delta^1\Delta^{15}N(D)$, as measured directly from the $^{15}$N,$^1$H IS-TROSY spectrum, is not a neat differential isotope effect. Rather, it is modified by the difference between the $^1J_{NH(E/Z)}$ coupling constants for the *E* and *Z* amide protons in semideuterated isotopomers because the chemical shift of the TROSY resonance is away from the corresponding HSQC resonance by half of the one-bond scalar coupling constant in both $^1$H and $^{15}$N dimensions (Figure 1, top panel). These one-bond scalar couplings can be accurately measured by $^{15}$N-coupled $^{15}$N,$^1$H HSQC experiments (see the Supporting Information) with the yCD NMR spectroscopic sample in 3:1 $H_2O/D_2O$. The result shows that for all side-chain amides, except for Asn51, $^1J_{NHE\{DZ\}}$ of $^{15}$NH$^E${D$^Z$} is 1–4 ppb larger than $^1J_{NHZ\{DE\}}$ of $^{15}$NH$^Z${D$^E$} in the $^1$H dimension at the 900 MHz field, which is commensurate with 10–

  

**Table 1.** Differential secondary protium/deuterium isotope effects and corresponding H-bond patterns of side-chain carboxamides in yCD.

| Residues | $\Delta^1\Delta^{15}N(D)$[a] (ppb) | $\Delta^2\Delta^{13}C'(ND)$[b] (ppb) | H-bond patterns[c] |
|---|---|---|---|
| Gln12 | 109 | 37 | $N–H^E\cdots O^{\delta1}$ of Asp16 (2.88/3.11 Å; 135/164°)[d] |
| Asn39 | 65 | 36 | $C{=}O^{\delta1}\cdots H–N^{bb}$ of Lys41 (2.75/3.03 Å; 122/157°) $C{=}O^{\delta1}\cdots H–N^{bb}$ of Asp42 (2.87/4.24 Å; 146/140°) |
| Asn40 | 103 | 41 | $N–H^E\cdots O^{\delta1}$ of Asp81 (2.86/2.89 Å; 171/168°) $N–H^Z\cdots O{=}C^{bb}$ of Thr82 (3.22/3.28 Å; 137/132°) $C{=}O^{\delta1}\cdots H^{\gamma1}–O^{\gamma1}$ of Thr83 (2.68/2.74 Å; 166/141°) |
| Asn51 | −18/−**4** | 57/**23** | $N–H^E\cdots$O2 of IPy (2.90/2.92 Å; 171/169°) $N–H^Z\cdots O^{\delta1}$ of Asp155 (2.90/2.92 Å; 162/162°) $C{=}O^{\delta1}\cdots H–N^{bb}$ of Arg53 (2.84/2.88 Å; 158/156°) |
| Gln55 | 128/**41** | 57/**17** | $N–H^E\cdots O^{\varepsilon2}$ of Glu28 (2.87/2.87 Å; 156/157°) $C{=}O^{\varepsilon1}\cdots H–N^{bb}$ of Gln55 (2.69/2.77 Å; 144/143°) |
| Asn70 | 84 | 37 | $N–H^E\cdots O{=}C^{bb}$ of Arg48 (2.77/2.83 Å; 172/176°) |
| Asn111 | 125 | 40 | $N–H^E\cdots O^{\varepsilon2}$ of Glu119 (2.90/2.94 Å; 162/161°) |
| Asn113 | 231/**260** | 39/**24** | $N–H^E\cdots O^{\varepsilon1}$ of Glu110 (2.57/2.62 Å; 158/166°)[d] $N–H^Z\cdots O{=}C^{bb}$ of Lys138 (3.09/3.14 Å; 154/146°)[d] |
| Gln123 | 53 | 35 | $N–H^E\cdots O{=}C^{bb}$ of Glu119 (2.94/3.64 Å; 146/129°) |
| Gln143 | 64 | 33 | $N–H^E\cdots O^{\eta}$ of Tyr126 (3.02/3.06 Å; 130/120°)[d] |
| Gln150 | 54 | 37 | no H bond |

[a] $\Delta^1\Delta^{15}N(D) = {}^1\Delta^{15}N(D^E) - {}^1\Delta^{15}N(D^Z)$, difference in one-bond H/D isotope effects on carboxyamide $^{15}N$ chemical shifts, where *E* stands for the *trans* position and *Z* the *cis* position of side-chain amide protons with respect to the carboxyamide oxygen. The values were measured directly from the 2D $^{15}N,^1H$ IS-TROSY spectrum without correction for differential $^1J_{NH(E/Z)}$ scalar coupling constants. The bold numbers include the contributions from trans-H-bond isotope effects. The standard error in repeated measurements is less than 5 ppb and RMSD to the mean is about 2 ppb; [b] $\Delta^2\Delta^{13}C'(ND) = {}^2\Delta^{13}C'(ND^E) - {}^2\Delta^{13}C'(ND^Z)$, difference in two-bond H/D isotope effects on carboxyamide $^{13}C'$ chemical shifts, where *E* stands for the *trans* position and *Z* stands for the *cis* position of side-chain amide protons with respect to the carboxyamide oxygen. The magnitudes that result from modifications of trans-H-bond isotope effects are in bold. The standard error in repeated measurements is less than 5 ppb and RMSD to the mean is about 2 ppb; [c] H bonds A–H···B involving the carboxyamide group of individual Asn/Gln residues in yCD derived from the 1.14 Å resolution crystal structure (PDB ID code: 1P6O); A designates the hydrogen donor and B the acceptor, followed by distances [Å] between heavy atoms A and B in two subunits with the corresponding H-bond angles in degrees; bb superscripted stands for protein backbone; [d] H bonds are formed only if positions of the nitrogen and oxygen atoms of the carboxyamide moiety are swapped in the crystal structure.

40 ppb in the $^{15}N$ dimension; repeated measurements essentially gave the same result. Because the magnitude of $^1J_{NH\{DZ\}}$ for $^1H^E$ is generally 1–4 Hz larger than that of $^1J_{NHZ\{DE\}}$ for $^1H^Z$, the differential $\Delta^1\Delta^{15}N(D)$ isotope effects are apparently "enhanced" by $(|{}^1J_{NHE\{DZ\}}| - |{}^1J_{NHZ\{DE\}}|)/2$, that is, 0.5–2.0 Hz (5–20 ppb at the $^{15}N$ frequency of 90 MHz). Asn51 is the sole exception and its $^1J_{NHE\{DZ\}}$ is slightly smaller (2 ppb) than $^1J_{NHZ\{DE\}}$; this is likely due to the very strong H bonding and charge effect through its *Z* proton. Because the differences of paired one-bond scalar coupling constants are quite uniform and relatively small at ultrahigh magnetic fields as measured with yCD, variations in apparent $\Delta^1\Delta^{15}N(D)$ from IS-TROSY in essence manifest the same changes in neat differential isotope effects caused by configuration, H bonding, charge effects, etc. For the sake of simplicity, we will not further discuss the enhancement of the differential isotope effects by the small difference in the scalar coupling constants.

### Differential two-bond H/D isotope effect on side-chain carboxamide $^{13}C'$ chemical shift

It has long been documented that the magnitude of isotope effects decreases rapidly with increasing number of bonds that separate the observed nucleus and the isotope-substituted position.[15] In protein backbones, however, the amide H/D isotope effects on two-bond $^{13}C'$ chemical shifts, $^2\Delta^{13}C'(ND)$, are surprisingly large, and range from 100 to 200 ppb.[11–12] In contrast, the two-bond isotope effects on $^{13}C^\alpha$, $^2\Delta^{13}C^\alpha(ND)$, are generally less than 100 ppb but are sensitive to the backbone conformation.[10] Traditionally, the large backbone $^2\Delta^{13}C'(ND)$ isotope effects are used for resonance assignments of peptides[25–26] and small proteins.[27–28] These two-bond isotope effects are also considered to be correlated with intraresidual H bonds in antiparallel β sheets, as demonstrated in the small protein BPTI,[29] although the reported magnitude falls into a rather narrow range, 60–90 ppb, in this case. The backbone amide proton of a residue is in the *trans* configuration with respect to the carbonyl oxygen of the preceding residue, which is characterized by the positive two-bond scalar coupling constant, $^2J_{HC'}$, between the amide proton and carbonyl carbon. Similarly, one of geminal protons in a side-chain carboxamide is in the *trans* configuration and shows a positive $^2J_{HC'}$ coupling constant as in the backbone, but the other is in the *cis* configuration and is characterized by a negative $^2J_{HC'}$ coupling constant.[30] This feature has been used for the stereospecific resonance assignment of side-chain amide protons in small proteins[31] and larger ones as well.[13] In side-chain carboxamide moieties of Asn/Gln residues, for the same reason of differential conjugative interactions and thus stretching frequencies, the magnitude of $^2\Delta^{13}C'(ND^E)$ from the *E* position is larger than $^2\Delta^{13}C'(ND^Z)$ from the *Z* position. As a result, the differential two-bond isotope effects, $\Delta^2\Delta^{13}C'(ND) = {}^2\Delta^{13}C'(ND^E) - {}^2\Delta^{13}C'(ND^Z)$, are expected to be positive too. The magnitude of $\Delta^2\Delta^{13}C'(ND)$ can be readily measured from the 2D IS-TROSY-H(N)CO spectrum (Figure 1 B).[13] It is worth noting that unlike $\Delta^1\Delta^{15}N(D)$, the magnitude of $\Delta^2\Delta^{13}C'(ND)$, as measured from the 2D IS-TROSY-H(N)CO spectrum, represents neat differential isotope effects with no contribution from scalar couplings. The $\Delta^2\Delta^{13}C'(ND)$ values of 11 Asn/Gln residues in yCD are indeed all positive (Table 1), in spite of the diversity in H-bonding interactions and charge effects among individual side-chain

  

amides. The influences of H bonding and/or charges appear to be largely attenuated over two bonds. Those side-chain amides with one of their geminal protons that are involved in H bonding with a negatively charged group, such as the carboxylate of an Asp/Glu residue, have slightly larger isotope effects, but the magnitudes of these two-bond differential isotope effects all fall into a narrow range of 33–57 ppb. The result indicates that $\Delta^2\Delta^{13}C'(ND)$ can be used for the configuration assignment of side-chain amides.

### Trans-hydrogen-bond H/D isotope effects

In a very recent publication, we reported the first detection of bifurcated hydrogen bonds by NMR spectroscopy by trans-H-bond H/D isotope effects.[32] Specifically, in the 1:1 $H_2O/D_2O$ solvent mixture, the resonances of side-chain $^{15}N,^1H^E\{D^Z\}$ of Asn51, the backbone amide of Asn113, and the side-chain $^{15}N,^1H^E\{D^Z\}$ of Asn113 show doublets in the $^1H$ dimension, which are caused by H/D isotope effects from the backbone amide protons of Gly63, Val112, and a bound water molecule, respectively, across H···O···H type of bifurcated H bonds.[32] Unexpectedly, the backbone amide resonance of either Gly63 or Val112 appears as a singlet; this indicates that the observed trans-H-bond isotope effects are asymmetrical. As such, the 2D $^{15}N,^1H$ IS-TROSY spectrum per se does not seem to identify both residues involved in the bifurcated H bonds. The two amide protons that are linked to each other in the H···O···H bifurcated H-bonding network, however, are close enough in space ($<4$ Å) so that their correlation can be exclusively established in the NOESY spectrum under the highly deuterated background in concert with the information from trans-H-bond isotope effects. Figure 2 shows a region of the 2D $^1H,^1H$ projection of the 3D $[^{15}N,^1H]$-IS-TROSY-dispersed-NOESY spectrum of yCD together with the corresponding 2D $^{15}N,^1H$ IS-TROSY spectrum. The weaker component (upfield) of the backbone amide resonance of Asn113 shows a cross peak with the backbone amide proton of Val112 in the NOESY spectrum, whereas the stronger component (downfield) does not; this indicates that the former is the resonance that corresponds to the protonated isotopomer and the latter is the deuterated isotopomer. This is consistent with the conclusion that is based on the spectral comparison with two yCD samples in 1:1 $H_2O/D_2O$ and in 95:5 $H_2O/D_2O$, respectively.[32] Interestingly, the chemical shift for the backbone amide proton of Val112 from the NOE cross peak that links the backbone amide proton of Asn113 (Figure 2B) is not exactly the same as the corresponding resonance in the $^{15}N,^1H$ IS-TROSY spectrum (Figure 2A), but rather it is found at about 10 ppb towards the upfield. This difference must be caused by the trans-H-bond H/D isotope effects, $^{2h}\Delta^1H$, from the backbone amide of Asn113, that is, the chemical shift of the Val112 resonance in the IS-TROSY spectrum corresponds approximately to the isotopomer that the backbone amide of Asn113 is deuterated because the protonated component is expected to be weaker, whereas the chemical shift of the Val112 cross peak in the NOESY spectrum must correspond exactly to the protonated component. In other words, combined with the IS-TROSY spectrum, the IS-TROSY-dispersed NOESY spectrum provides not only the valuable correlation information between the two amide protons that are connected through bifurcated H bonds, but also the magnitude and sign of the $^{2h}\Delta^1H$ isotope effect even when it is smaller than the line width. The sign of the $^{2h}\Delta^1H$ isotope effect for Val112 is negative, but the small $^{3h}\Delta^{15}N$ isotope effect through the Val112-N–H···O···H/D-Asn113 hydrogen bonds for Val112 appears positive, although the magnitude is very small. No NOE was observed between the backbone amide proton of Gly63 and the side-chain amide protons of Asn51 within the limited measuring time, presumably because the relative population of the fully protonated or each semideuterated isotopomer of a side-chain amide is only about half of the corresponding protonated backbone amide in the mixture solvent, and the spin diffusion within the nearby protonated ligand is expected to be a negative factor to the expected NOE. Nonetheless, in principle, such NOEs involving side-chain amide protons should be detectable and provide valuable correlation information in concert with trans-H-bond isotope effects for the assignment of Asn/Gln rotamers.

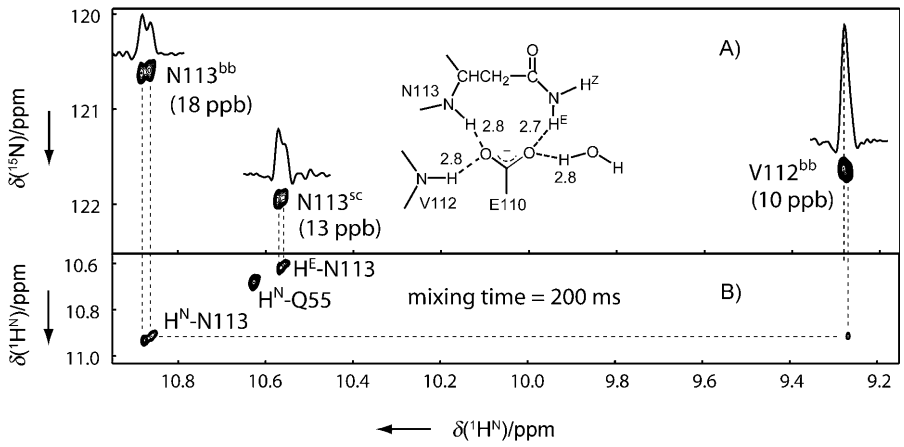


**Figure 2.** Regions of A) the 2D $^{15}N,^1H$ IS-TROSY spectrum and B) the 2D projection of 3D $^{15}N,^1H$ IS-TROSY-dispersed NOESY spectrum of yCD with u-$^2H/^{13}C/^{15}N$ labeling in 1:1 $H_2O/D_2O$. The spectrum was recorded by using a Bruker Avance 900 MHz NMR spectrometer. Experimental and data processing conditions were the same as in Figure 1. Inset in panel A) shows the suggested hydrogen-bonding network of Asn113, which is derived from the 1.14 Å crystal structure of yCD (PBD ID code: 1P6O) after flipping the side-chain oxygen and nitrogen positions.

Interestingly, neither the magnitudes nor the signs of the two-bond isotope effect, $^{2h}\Delta^1H$, and the three-bond isotope effect, $^{3h}\Delta^{15}N$, that are transmitted through $^{15}N$–H···O···H/D bifurcated H bonds are uniform, which probably reflects the diversity in geometries and/or electronic features of the corresponding H-bonding networks. In addition, a closer inspection reveals that the

  

$^1H^E$ resonance of Gln55 also shows doublets in both $^1H$ and $^{15}N$ dimensions of the IS-TROSY spectrum. Because it forms bifurcated H bonds together with the $H^{\varepsilon 2}$ of His50 to the $O^{\varepsilon}$ atom of Glu28 in the crystal structure, the splittings are most likely due to trans-H-bond isotope effects with positive 12 ppb of $^{2h}\Delta^1H$ in the $^1H$ dimension and a small positive $^{3h}\Delta^{15}N$ in the $^{15}N$ dimension (Figure 3). Furthermore, the four-bond H/D isotope effect on the side-chain carboxamide carbon, $^{4h}\Delta^{13}C'$, which is transmitted through $^{13}C'$-N–H···O···H/D bifurcated H bonds, can be observed in the 2D H(N)CO-IS-TROSY spectrum (Figure 4). The signs of $^{4h}\Delta^{13}C'$ for all the three bifurcated H bonds are positive. They are those between the side-chain amides of Asn51, Gln55 and Asn113 and the backbone amide of Gly63 through the carbonyl oxygen (O2) of the ligand, the side-chain $H^{\varepsilon 2}$ of His50 through the side-chain $O^{\varepsilon}$ of Glu28 and a water molecule through the side-chain $O^{\varepsilon}$ of Glu110, respectively. The sign of $^{4h}\Delta^{13}C'$ for the backbone amide of Asn113 due to the bifurcated H bond of the backbone amide of Val112 through the carboxyl oxygen of Glu110 also appears positive, although the magnitude is negligibly small (Figure 4). The modified differential isotope effects that are due to the trans-H-bond isotope effects are also listed in Table 1 (bold text).

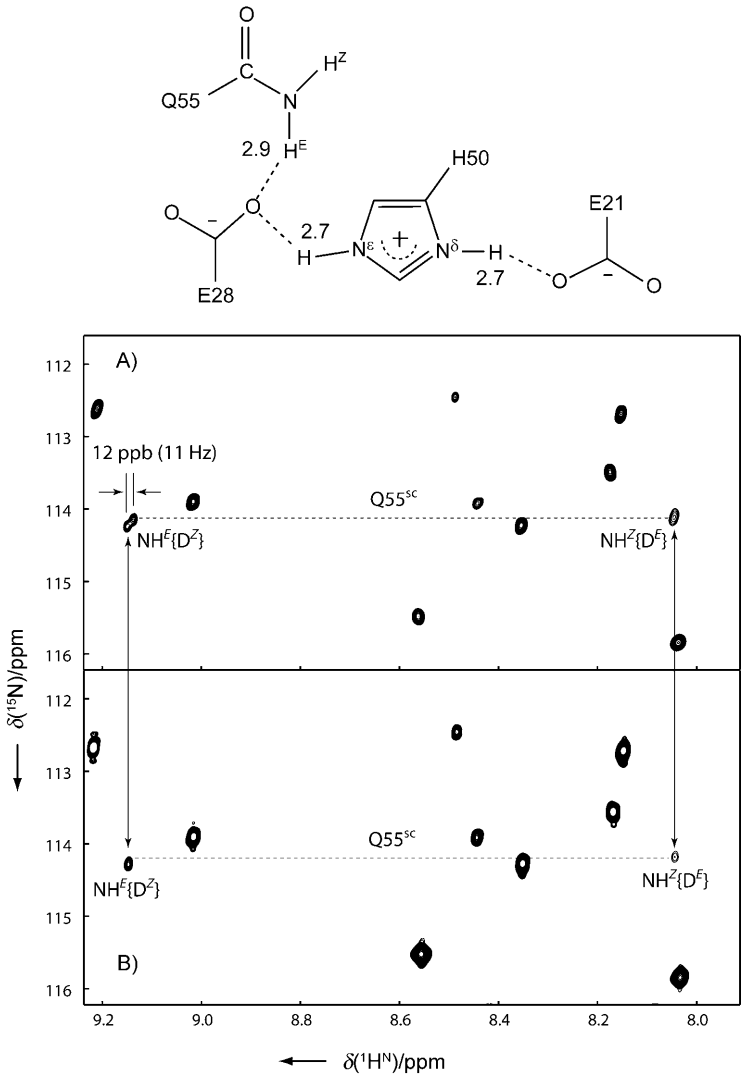


**Figure 3.** Regions of the 2D $^{15}N$,$^1H$ IS-TROSY spectra of u-$^2H$/$^{13}C$/$^{15}N$ labeled yCD in A) 1:1 $H_2O/D_2O$ and B) 95:5 $H_2O/D_2O$. The spectra were recorded by using a Bruker Avance 900 MHz NMR spectrometer. Experimental and data processing conditions were the same as in Figure 1. The doublets of Gln55-$NH^E\{H^Z\}$ resonance were caused by trans-H-bond H/D isotope effects mediated by the bifurcated H bond of His50-$H^{\varepsilon}/D^{\varepsilon}$ as illustrated in the top diagram.

### Correlation with H-bonding network

Whereas the narrow range of positive differential two-bond $\Delta^2\Delta^{13}C'(ND)$ isotope effects is useful for the configuration assignment of side-chain amides, the large variations in the differential one-bond $\Delta^1\Delta^{15}N(D)$ isotope effects can be correlated with H bonds that are involved in the side-chain amides. Two crystal structures of yCD in complex with a transition state analogue (PDB ID codes: 1UAQ and 1P6O) at the resolutions of 1.6 Å[33] and 1.14 Å,[34] respectively, have been published. Because the 1P6O structure is of much higher resolution, we will mainly use this as the reference to illustrate the contraventions and uncertainties in the H-bonding interactions of side-chain carboxamides, as revealed by measured H/D isotope effects. In the crystal structure, side-chain amide protons of Gln12, Asn39, Asn113, Gln123, Gln143, and Gln150 are exposed to the solvent and make no, or weak H-bonding interactions to potential acceptors. Except for Gln12 and Asn113, all these solvent-exposed amides, as evidenced by their sharp and poorly dispersed resonances in the 2D $^{15}N$,$^1H$ correlation spectra, render uniform magnitudes of $\Delta^1\Delta^{15}N(D)$ and $\Delta^2\Delta^{13}C'(ND)$ that range from 52–65 ppb and 33–37 ppb, respectively; this reflects the neat conjugative difference between the *E* and *Z* configurations. Surprisingly, the $\Delta^1\Delta^{15}N(D)$ effects of Gln12 and Asn113 are about two times (109 ppb) and four times (231 ppb), respectively, larger than those of other residues within this group. Apparently, there must be contributions from other factors. Both theoretical calculations[35] and experimental measurements[10] with model compounds and small proteins indicate that one-bond H/D isotope effects on $^{15}N$ chemical shifts, $^1\Delta^{15}N(D)$, depend on H-bonding strengths (in terms of bond lengths and angles) and charges, which arouse electric field effects in the vicinity of the amide proton.[16–18] It has been widely accepted that upon H bonding, the potential of stretching vibrations become more asymmetrical with a lower zero-point energy for a deuterium in comparison with a protium; this leads to an enlarged difference in the bond lengths between $^{15}N$–H and $^{15}N$–D, and thus a larger isotope effect results.[5] Moreover, ionization could greatly affect H bonding; a positively charged donor and/or a negatively charged acceptor will strengthen the H bond by virtue of an increased attraction in electron densities associated with the acceptor and donor.[7] As such, negative charges at the H/D acceptor site, such as the carboxyl oxygen atoms of an acidic residue,

  

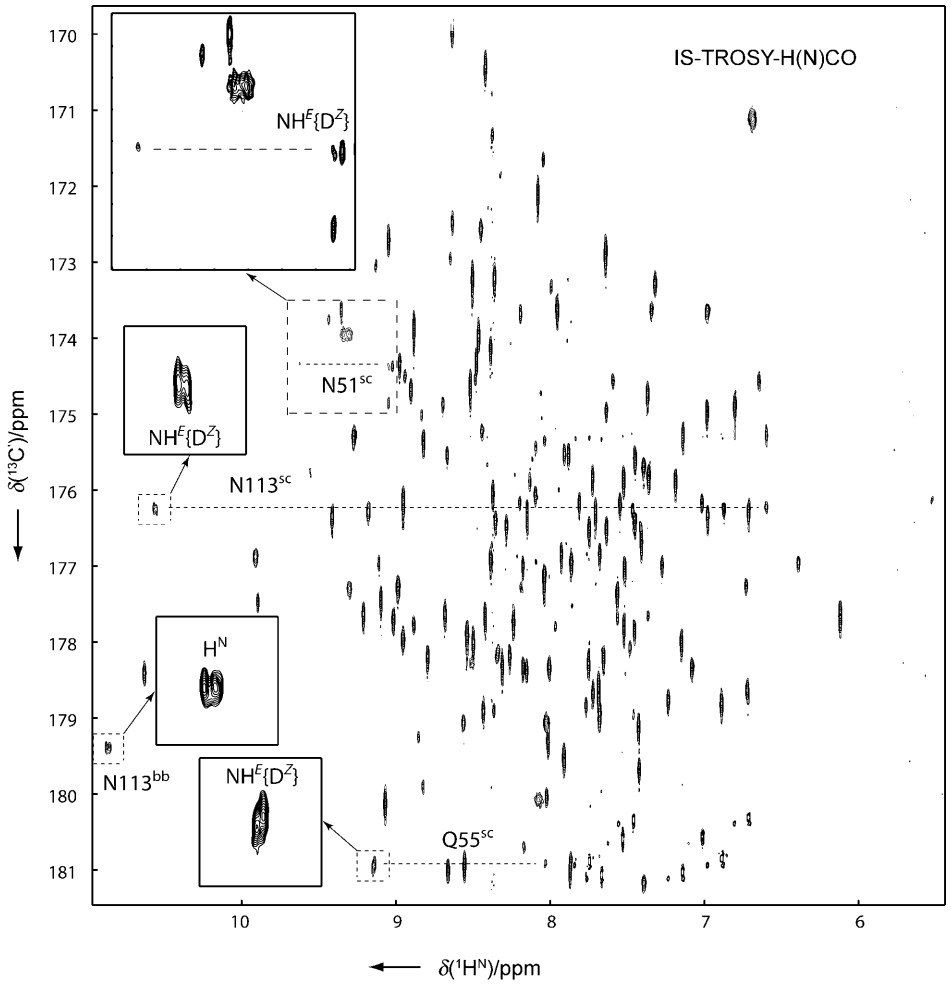


**Figure 4.** The 2D IS-TROSY-H(N)CO spectrum of u-$^2$H/$^{13}$C/$^{15}$N-labeled yCD in 1:1 $H_2O/D_2O$. The spectrum was recorded by using a Bruker Avance 900 MHz NMR spectrometer. The doublet Asn/Gln side-chain amide cross-peaks, which are enclosed with dashed squares and enlarged with solid squares, were caused by trans-H-bond isotope effects $^{2h}\Delta^1$H and $^{4h}\Delta^{13}$C′. The spectrum was recorded with 128 scans and a 1.8 s delay time, $t_{1max}(^{13}C) = 71$ ms and $t_{2max}(^1H^N) = 285$ ms; this resulted in the experimental time of 41 h. Before Fourier transformation, the raw data were zero-filled; this resulted in a 1.0 Hz digital resolution in the indirect dimension.

strengthen the H bond through hyperconjugative interactions with the amide moiety and give rise to more significant isotope effects. Therefore, the unexpectedly large $\Delta^1\Delta^{15}$N(D) values of Gln12 and Asn113 most likely result from H bonding and charges. Indeed, if the positions of the nitrogen and oxygen atoms in the side-chain carboxamides are flipped, the $^1H^E$ of Gln12 might form a H bond with the carboxylate group of Asp16 and the $^1H^E$ of Asn113 might form a H bond with the carboxylate group of Glu110 (Table 1). The H bond that involves the $^1H^E$ of Asn113 is strong, with a short bond length (~2.60 Å between the heavy atoms) and a nearly ideal bond angle ($\geq 160^\circ$). However, the H bond that involves the $^1H^E$ of Gln12 is rather weak with a longer bond length and smaller bond angle. This is also indicated by its sharp resonances and the chemical shift, which is characteristic of a flexible side-chain amide. Therefore, the large $\Delta^1\Delta^{15}$N(D) magnitude for Gln12 is likely mainly caused by the negative charge of Asp16, which enhances the isotope effect by at least 40 ppb, and the much larger magnitude for Asn113 must be due to the combined result of the charge and a strong H bond with Glu110. The correlations between the large $\Delta^1\Delta^{15}$N(D) magnitudes and charge and/or H-bond strength for Gln12 and Asn113 are confirmed by the observation of large $\Delta^1\Delta^{15}$N(D) magnitudes for Asn40 (103 ppb), Gln55 (128 ppb) and Asn111 (125 ppb), the $^1H^E$ atoms of which form H bonds with the negatively charged carboxyl oxygen atoms of Asp81, Glu28, and Glu119, respectively, with similar bond lengths (~2.9 Å) and angles (155–170°). Interestingly, the $^1H^Z$ (not $^1H^E$) of Asn51 forms a H bond with the carboxyl oxygen of Asp155 (negatively charged), which apparently overwhelms the combined contributions from differential configurations and differential $^1J_{NHE\{DZ\}}/^1J_{NHZ\{DE\}}$ coupling constants as well as the neutral H bond between the $^1H^E$ of Asn51 and the O2 atom of the ligand, and makes its $\Delta^{15}$N($D^Z$) larger than $\Delta^{15}$N($D^E$)—thus a slightly negative value of $\Delta^1\Delta^{15}$N(D)—because the contribution from the charged H bond is at least two-times larger in magnitude than that of the configuration effects. On the other hand, the $^1H^E$ of Asn70 forms a neutral H bond with the backbone carbonyl oxygen of Arg48 and the magnitude of its $\Delta^1\Delta^{15}$N(D) is 84 ppb, which is 20–30 ppb larger than those involved in no, or very weak H bonding, but at least 20 ppb smaller than those involved in H bonds with negatively charged acceptors. For the side-chain amide of Gln123, its $^1H^E$ could form a weak H bond to the backbone carbonyl oxygen (no charge) of Glu119 with a bond length of 2.94 Å in one subunit of the crystal structure, but the corresponding distance is as long as 3.64 Å in the other subunit, which is unlikely to form a H bond. This is supported by the unstructured character of its side-chain resonances. The $^1H^E$ of Gln143 could form a weak H bond to the $O^\eta$ of Tyr126 if the side-chain N/O atom positions of the former are swapped. The side-chain amide of Gln150 does not form any H bond in the crystal structure. The H-bonding contributions to $\Delta^1\Delta^{15}$N(D) through the side-chain carboxamide oxygen appear rather small. For instance, the side-chain oxygen of Asn39 forms bifurcated H bonds to both backbone amides of Lys41 and Asp42, but its $\Delta^1\Delta^{15}$N(D) mag-

  

nitude is only 65 ppb, similar to those without or with weak H bonding.

Based on the above analysis on the isotope effects listed in Table 1, an empirical quantification emerges as described in Equation (1) that contains additive contributions to differential one-bond H/D isotope effects on $^{15}N$ chemical shifts of side-chain amides:

$$\Delta^1\Delta^{15}N(D) \equiv {}^1\Delta^{15}N(D^E) - {}^1\Delta^{15}N(D^Z) = \Delta_c + \Delta_j + \Delta_h + \Delta_e + \Delta_o + \Delta_a \quad (1)$$

The first two terms are intrinsic: $\Delta_c$ is the contribution of configurational effects with a positive magnitude of 40–45 ppb and $\Delta_j$ is the contribution of differential $^1J_{NH^E\{DZ\}}/^1J_{NHZ\{DE\}}$ coupling constants normally with a positive magnitude of 5–20 ppb (at the 90 MHz field). The third term, $\Delta_h$, reflects the contributions from H-bonding interactions; a weak H bond can account for 10 ppb and a normal one for 30 ppb, and the sign is positive if $^1H^E$ is involved, but negative if $^1H^Z$ is involved. The term $\Delta_e$ represents the contribution of charges involved in H bonds, that is, negatively charged Asp/Glu side-chain carboxyl oxygen atoms as hydrogen acceptors in this work. It is about 40 ppb for a weak H bond. However, $\Delta_e$ might be over 140 ppb for a strong H bond with a positive sign if $^1H^E$ is involved, but negative if $^1H^Z$ is involved in the H bond. The term $\Delta_o$ is the H-bonding contribution through the oxygen atom of a side-chain carboxamide and is normally small, only about 10 ppb. The last term, $\Delta_a$, is the contribution from trans-H-bond isotope effects, which can vary significantly, as described earlier. In brief, the magnitude of $\Delta^1\Delta^{15}N(D)$ in side-chain amides is intricately governed by the differential configurations but significantly modified by H-bonding interactions, particularly those with charged H-bond acceptors, such as carboxyl oxygen atoms of Asp/Glu residues. Significant deviations in $\Delta^1\Delta^{15}N(D)$ from the nominal values of solvent-exposed, flexible side-chain amides (50–60 ppb at the 90 MHz field) are strongly indicative of H bonding and charges, and can be directly correlated with H-bonding networks.

It is noteworthy that typically only the $^1H^E$ or $^1H^Z$, but not both, of a side-chain amide forms a H bond with a negatively charged acceptor, because the proximity of two negatively charged groups is energetically unfavorable. On the other hand, both the $^1H^E$ and $^1H^Z$ of a side-chain amide could form neutral H bonds simultaneously, which might result in a small neat contribution to $\Delta^1\Delta^{15}N(D)$. There is, however, not such a case in yCD. Perhaps one would expect a smaller $\Delta^1\Delta^{15}N(D)$ in comparison with non-H-bonded situations if only $^1H^Z$ forms a neutral H bond. Unfortunately, there is not such an example in yCD either. This speculation must await the observation in more proteins with high-resolution structures.

#### Rotamer correction

As described in the Introduction section, a rather high percentage of side-chain amide rotamers is incorrectly assigned in both crystal and NMR structures of proteins. Such errors are found even in ultrahigh-resolution crystal structures, for example, the 0.85 Å resolution crystal structure of the 122-residue acutoaemolysin.[36] Of the eleven side-chain amides of this protein, three have incorrect rotamers. Residual dipolar coupling (RDC) data have been used for the identification of erroneous side-chain amide rotamer assignments in 16 high-resolution crystal structures of hen egg-white lysozyme.[37] Of the 146 rotamers that were assigned based on the NMR spectroscopic data, 26 are inconsistent with those in the crystal structures. Whereas RDC analysis is very powerful for the correction of side-chain amide rotamer assignment errors, acquisition of RDC data is much more complicated than the measurement of differential isotope effects. Moreover, the $^1H$–$^1H$ RDC data for side-chain amides are difficult to obtain for large proteins, because of line broadening due to strong dipole–dipole interactions, unless the IS-TROSY strategy is adopted.[13,14]

The differential secondary isotope effects of side-chain amides provide a simple means for the correction of the erroneous rotamer assignments. Based on the analysis of the differential secondary isotope effects as described above, the side-chain $^1H^E$ proton of Asn113 forms a strong H bond with charged groups. The H bonding of Asn113 as revealed by differential isotope effects is inconsistent with the side-chain amide rotamer assignments for this residue in both subunits of the 1.14 Å resolution crystal structure. Although the side-chain amide of Gln12 can form a transient H bond with the carboxyl group of Asp16, it is mobile. Consequently, the side-chain amide Gln12 adopts one conformation in subunit A of the 1.14 Å crystal structure, but another in subunit B. The rotamer assignments of all other Asn/Gln side-chain amides are consistent with the differential isotope effects. In all, this analysis identifies two rotamer assignment errors in this high-resolution crystal structure. For the 1.6 Å resolution crystal structure the rotamer assignment for Asn113 is correct for both subunits. The conformation of the side-chain amide of Gln12 in subunit A is completely different from that in subunit A of the 1.14 Å crystal structure, but that in subunit B is 180° rotated from that in subunit B of the 1.14 Å crystal structure, that is, a flipping of the rotamer; this underscores the mobility of the side-chain amide. The flipping of the side-chain amide in the 1.6 Å resolution crystal structure allows it to form a hydrogen bond with the carboxyl group of Asp16. The side-chain amide rotamers of Gln55, Asn70, and Asn111 are all inconsistent with the differential isotope effects—they require flipping to form H bonds. In total, there are six side-chain amide rotamer assignment errors in this crystal structure as listed in Table 2.

Because of the frequent errors in side-chain amide rotamer assignment in protein structures, computational approaches have been developed for correcting the errors.[2,4,36] In particular, two web servers are available for the identification and correction of such errors, one server (MolProbity, http://molprobity.biochem.duke.edu/) uses steric clashes after the addition of hydrogen atoms as a criterion for identifying such errors[38] and the other (NQ-Flipper, http://flipper.services.came.sbg.ac.at) uses an empirical potential as a criterion for identifying such errors.[36] We submitted both yCD crystal structures to the web services to check their side-chain rotamers; the results are listed in Table 2. Both MolProbity and NQ-Flipper identified

  

**Table 2.** Asn/Gln side-chain rotamer errors in yCD crystal structures as recognized by differential isotope effects and the programs MolProbility and NQ-Flipper.

| PDB ID | Subunit | NMR | MolProbility | NQ-Flipper |
|---|---|---|---|---|
| 1P6O | A | Asn113 | Gln12,[a] Asn113 | Gln12,[a] Asn113 |
| | B | Asn113 | Asn113 | Asn113, Gln123, Gln143 |
| 1UAQ | A | Gln55, Asn70, Asn111 | Gln55, Asn70, Asn111, Gln143 | Asn70, Asn111, Gln143 |
| | B | Gln55, Asn70, Asn111 | Asn39, Gln55, Asn70, Asn111, Gln123, Gln143 | Gln12,[a] Asn39, Asn70, Asn111, Gln143, Gln150 |

[a] According to the NMR and MD simulation data, the side-chain amide of Gln12 is mobile and can adopt a variety of rotamer conformations.

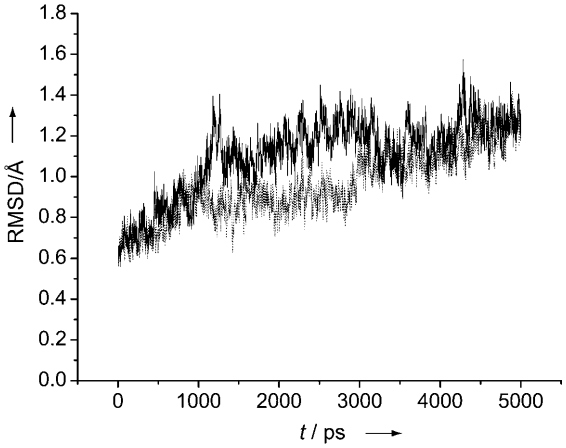


**Figure 5.** Evolution of the $C^{\alpha}$ RMSDs of residues 15–158 of subunit 1 (——) and subunit 2 (-----) from those of the 1.14 Å resolution crystal structure during the entire MD simulation period.

three rotamer errors in the 1.14 Å crystal structure, including one for Gln12, which is mobile. However, NQ-Flipper also identified two residues (Gln123 and Gln143) in subunit B for rotamer flipping, but such flipping is not necessary for both residues upon visual inspection. With respect to the 1.14 Å structure, MolProbity recognized all six rotamer assignment errors that were identified by the differential isotope effects and also recommended an additional four residues for flipping that were deemed unnecessary upon visual inspection. NQ-Flipper correctly identified only four rotamer assignment errors. The two rotamer errors for Gln55 were not identified, but five Asn/Gln residues with apparently correct rotamers were recommended for rotamer flipping. With respect to the two yCD structures, MolProbity did a better job in identifying side-chain rotamer errors than NQ-Flipper, but both programs recommended some rotamers for flipping deemed unnecessary upon visual inspection.

To better understand side-chain amide flipping, we performed a 5 ns molecular dynamics (MD) simulation of the complex of yCD with the transition state analogue, which was essentially an extension of a previous MD analysis of yCD[39] with a newer version of the Amber MD package (version 8)[40] and force field (ff03).[41] It should be noted that no rotamer error correction was made to the initial structure for the MD simulation. The data analysis was based on individual subunits to obtain better statistics. Figure 5 shows the time evolution of the $C^{\alpha}$ atom RMSDs of two subunits with the coordinates of the crystal structure as reference. The first eleven residues are not included in the analysis because the N-terminal segment is highly mobile as in the previous MD simulations. The average $C^{\alpha}$ RMSD over the 5 ns MD simulation is 0.96 Å for subunit 1 and 1.10 Å for subunit 2. The average mass-weighted RMSD for all heavy atoms is 1.49 Å for subunit 1 and 1.62 Å for subunit 2. The result indicates that the structural changes in the protein are not large, and the MD simulation is stable. Based on a trace-back RMSD analysis, the system reaches a stationary point at ~0.75 ns.

Further data analysis, which focused on the motions of the side-chain amide groups was performed on the trajectory extracted from the last 4 ns. The side-chain amide motions in this analysis were measured by the $\chi^2$ torsion angle ($C^{\alpha}$–$C^{\beta}$–$C^{\gamma}$–$O^{\delta}$) for Asn and the $\chi^3$ torsion angle ($C^{\beta}$–$C^{\gamma}$–$C^{\delta}$–$O^{\varepsilon}$) for Gln. The result is shown in Figure 6. It is clear that the side-chain amides of Gln12, Gln123, Gln143, and Gln150 can adopt a variety of rotamer conformations, as the torsion angles that define these rotamers vary widely in the MD simulation. The rapid motions of theses side-chain amides are consistent with their sharp NMR spectroscopic signals. Consequently, it is not meaningful to discuss the rotamer assignments and their errors. The side-chain amide of Asn39 in subunit 1 oscillates significantly around its torsion in the crystal structure but not in subunit 2. The side-chain amide of Asn113 flips in subunit 1 and remains in that conformation but oscillates significantly in subunit 2. The side-chain amides of Asn40, Asn51, Gln55, Asn70, and Asn111 behave like immobilized groups; this is consistent with their broader NMR spectroscopic signals, although the side-chain amide of Asn111 assumes one conformation in subunit 1 and another in subunit 2. In particular, the rotamer assignment of Gln55 is incorrect in the 1.6 Å resolution crystal structure based on the differential isotope effects, the MD simulation, the 1.14 Å resolution crystal structure, and the MolProbity server analysis, but the NQ-Flipper server could not pick up the rotamer assignment error for this residue.

## Conclusions

Protium/deuterium (H/D) isotope effects on chemical shifts can be transmitted either by covalent bonds or across hydrogen bonds and provide a sensitive means for studying H-bonding interactions, especially in large proteins in which trans-hydrogen-bond scalar couplings are too small to be measured. In this study, the configuration and H-bonding network of side-chain amides in a 35 kDa protein were determined by measuring differential and trans-H-bond H/D isotope effects with the IS-TROSY technique; this led to reliable recognition and correction of erroneous rotamers frequently found in protein structures. First, the differential two-bond isotope effects on carbonyl $^{13}C'$ shifts $\Delta^2\Delta^{13}C'(ND)$ provide a reliable means for the configuration assignment for side-chain amides because envi-

  

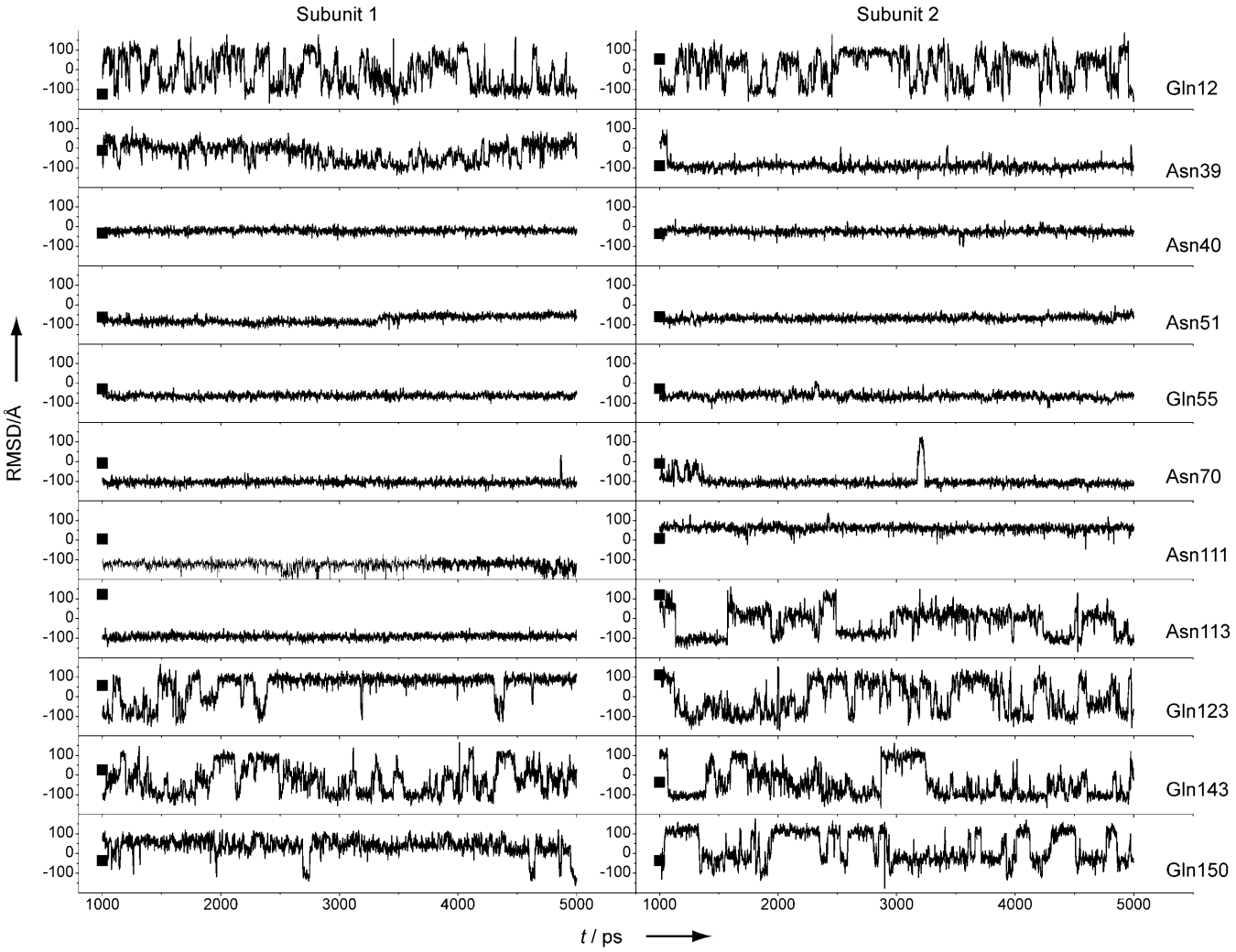


**Figure 6.** Variations of the torsion angles for the side-chain amides in the last 4 ns MD simulation. The torsion angles measured from the 1.14 Å resolution crystal structure are indicated by solid squares. The subunit identities are labeled at the top and residue identities on the left side.

ronmental effects (hydrogen bonds and charges, etc.) are largely attenuated over the two bonds that separate the carbon and hydrogen atoms and the isotope effects fall into a narrow range of positive values. Second and more importantly, the significant variations in the differential one-bond isotope effects on $^{15}N$ chemical shifts $\Delta^1\Delta^{15}N(D)$ can be correlated with H-bonding interactions, particularly those involving charged acceptors. The differential one-bond isotope effects are additive, with major contributions from intrinsic differential conjugative interactions between the *E* and *Z* configurations, H-bonding interactions, and charge effects. Furthermore, the pattern of trans-H-bond H/D isotope effects can be mapped onto more complicated H-bonding networks that involve bifurcated H bonds. Third, the correlations between $\Delta^1\Delta^{15}N(D)$ and H-bonding interactions afford a simple but effective means for the correction of erroneous side-chain amide rotamer assignments. Although several software programs and web-based services have been developed for the recognition and correction of erroneous side-chain amide rotamers, they are not always reliable, as demonstrated in the analysis of the side-chain amide rotamer assignments in the two high-resolution crystal structures of yCD. Very few experimental methods are available for this purpose. RDC data in conjunction with $^{15}N$ relaxation measurements have been used for correcting Asn/Gln rotamers of solution-phase NMR spectroscopic structures, but this method is laborious and applicable to only small proteins. In contrast, the rotamer correction through the differential isotope effects is not only robust but also simple and can be applied to large proteins.

## Experimental Section

**Sample preparation and experimental conditions**: The procedure for isotope labeling and purification of yCD has been described.[42] NMR spectroscopic samples were prepared by dissolving lyophilized yCD powder with phosphate buffer (100 mM potassium, pH 7.0; without isotope correction) in mixture solvents (either 95:5 $H_2O/D_2O$ or 1:1 $H_2O/D_2O$). $NaN_3$ (100 μM) and 2,2-dimethyl-2-silapentane-5-sulfonic acid (DSS; 20 μM as an internal NMR reference) were added. The volume of all samples was about 300 μL in Shige-

  

mi NMR spectroscopy microcells. Each NMR spectroscopic sample had yCD protein (~1.5 mM protomer) titrated with the transition state analogue 5FPy (20 mM). The samples in the mixture solvent were equilibrated at room temperature for at least a week before being measured. All NMR spectroscopic measurements were performed on a Bruker Avance 900 MHz NMR spectrometer at 25 °C by using a TCI cryoprobe with *z*-axis gradient and an automatic tuning/matching unit. The raw data were processed with NMRPipe,[43] and spectra were analyzed with NMRView.[44]

**Measurements of differential and trans-H-bond H/D isotope effects**: The $^{15}N,^{1}H$ IS-TROSY experiment selectively detected semideuterated isotopomers of side-chain amides.[13–14] As depicted in Figure 1, the resonance of the $^{15}N–H^{E}\{D^{Z}\}$ isotopomer has the $^{15}N$ chemical shift modified by the one-bond $^{1}\Delta^{15}N(D^{Z})$ isotope effect from the *Z* position and the $^{15}N–H^{Z}\{D^{E}\}$ isotopomer by $^{1}\Delta^{15}N(D^{E})$ from the *E* position. Because resonances of the fully protonated isotopomer, $^{15}NH_2$, have been filtered out, direct measurements of $^{1}\Delta^{15}N(D^{Z})$ and $^{1}\Delta^{15}N(D^{E})$ were not possible from $^{15}N,^{1}H$ IS-TROSY spectra. The differential one-bond isotope effects, $\Delta^{1}\Delta^{15}N(D) = {}^{1}\Delta^{15}N(D^{E}) - {}^{1}\Delta^{15}N(D^{Z})$, could be measured directly, although the values were modified by the differential $(|{}^{1}J_{NH^{E}\{D^{Z}\}}| - |{}^{1}J_{NH^{Z}\{D^{E}\}}|)/2$ scalar coupling constants between the *E* and *Z* protons (Figure 1). The magnitudes of one-bond scalar coupling constants, $|{}^{1}J_{NH^{E}\{D^{Z}\}}|$ and $|{}^{1}J_{NH^{Z}\{D^{E}\}}|$, were measured from a 2D $^{15}N,^{1}H$ HSQC spectrum without the use of broad-bond $^{15}N$ decoupling in the direct dimension. The yCD NMR spectroscopic sample used for this measurement was in 3:1 $H_2O/D_2O$ otherwise the same buffer conditions as for other yCD samples described in the last section were used. The ratio of $H_2O/D_2O$ was manipulated to obtain good signal intensities for both protonated and semideuterated isotopomers of side-chain amides while alleviating the potential complication caused by trans-H-bond isotope effects. The one-bond scalar coupling constants in side-chain amides were directly measured from the $^{1}H$ signal splittings of the corresponding semideuterated $^{15}NH\{D\}$ isotopomers in this $^{15}N$-coupled HSQC spectrum (Supporting Information). Similarly, the differential two-bond isotope effects, $\Delta^{2}\Delta^{13}C'(ND) = {}^{2}\Delta^{13}C'(ND^{E}) - {}^{2}\Delta^{13}C'(ND^{Z})$, were measured from the 2D IS-TROSY-H(N)CO spectrum of yCD (Figure 1 B). Unlike the one-bond isotope effects shown in Figure 1 A, the two-bond isotope effects in Figure 1 B were neat without any modification from scalar couplings, because no TROSY principle was adopted in the $^{13}C$ dimension of the 2D IS-TROSY-H(N)CO experiment. Trans-H-bond two-bond and three-bond H/D isotope effects on side-chain amide proton and $^{15}N$ chemical shifts, $^{2h}\Delta^{1}H$ and $^{3h}\Delta^{15}N$, respectively, which were mediated by H···O···H bifurcated H bonds,[32] were measured either from the $^{15}N,^{1}H$ IS-TROSY spectrum (Figure 3) or in combination with the IS-TROSY-dispersed NOESY spectrum (Figure 2; see the Supporting Information for the pulse sequence). The new observation of trans-H-bond four-bond isotope effects on side-chain $^{13}C'$, $^{4h}\Delta^{13}C'$, were obtained from the 2D IS-TROSY-H(N)CO spectrum (Figure 4).

Although the magnitude of certain differential isotope effects as measured above might be smaller than the linewidth in the indirect dimension, the large separation in the direct ($^{1}H$) dimension of the paired resonances of a side-chain amide makes measurement easy and accurate; this mimics the measurement of small scalar coupling constants in E.COSY-type experiments.[24] Indeed, duplicated measurements indicated that the standard error was as small as 5 ppb and the RMSD to the mean was only about 2 ppb. Markley and Loh have shown that amide D/H fractionation factors might be correlated to the strength of H binding in proteins.[45] The correlation was established by measuring the intensity of amide resonances with a set of protein NMR spectroscopic samples in solvent mixtures that had different ratios of $H_2O/D_2O$. The ratio, in principle, had little to do with the chemical shifts of individual resonances because solvent isotope effects on $^{15}N$ chemical shifts were very small.

**Molecular dynamics simulation**: MD simulation on the complex of yCD with the transition-state analogue was carried out essentially in the same way as previously described,[39] except that version eight of the Amber MD package and the Amber 03 force field[46] were used for this simulation. Briefly, the starting structure was taken from the 1.14 Å resolution crystal structure (PDB ID: 1P6O).[34] Hydrogen atoms were added with the Insight II program. All ionizable residues were assigned to their normal protonated state at pH 7.0 except for His50, which was set as the protonated form because its imidazole ring was hydrogen bonded to two carboxyl groups (Figure 3). The catalytic zinc ion was tetrahedrally coordinated with His62, Cys91, Cys94 and the transition state analogue. The sulfur atoms of Cys91 and Cys94 were deprotonated and His62 was in a deprotonated form and only $N^{\varepsilon}$ had a proton attached to it. Explicit bonds between the zinc atom and its ligands were used, and the force constants were the same as in our previous work.[39] The RESP charges of the zinc complex (Zn, His62, Cys91, Cys94 and the transition state analogue) were derived from a single-point quantum mechanics calculation (B3LYP/6-31 + G*). Glu64 was also included in the calculation because it might influence the charge distribution through a strong H bond.

The protein complex was solvated by ~17 000 TIP3P water molecules in a periodic box with a minimum distance of 12.5 Å between the protein and the walls of the periodic box and was neutralized by the addition of four $Na^{+}$ ions. Sander in Amber 8[40] and the ff03 force field were employed for the MD simulation. The system was first subjected to a two-stage energy minimization to eliminate steric clashes and two short MD runs for the system to reach the desired temperature and density. During the production MD run, the system was maintained at constant volume and temperature (300 K) by using Berendsen's weak-coupling method.[47] Bond lengths involving hydrogen atoms were constrained by the Shake algorithm.[48] The Particle–Mesh–Ewald method was used to evaluate long-range electrostatic interactions.[49] A cutoff of 8.0 Å was used for the nonbonded pair list, which was updated every 25 steps. Coordinates were saved every other picosecond. The simulation results were analyzed with the PTRAJ module in Amber 8.

## Acknowledgements

*This work made use of a Bruker Avance 900 MHz NMR spectrometer funded by Michigan Economic Development Corporation and Michigan State University. We thank Yan Wu for preparing NMR samples. The work was partially supported by NIH grant GM58221 (H.Y.). A.L. was a recipient of the New Faculty Awards at MSU.*

**Keywords:** configuration determination · hydrogen bonds · isotope effects · NMR spectroscopy · rotamer assignment

[1] T. E. Creighton, *Proteins: Structure and Molecular Properties*, 2nd ed., Freeman, New York, **1993**.
[2] J. M. Word, S. C. Lovell, J. S. Richardson, D. C. Richardson, *J. Mol. Biol.* **1999**, *285*, 1735–1747.
[3] H. M. Berman, J. Westbrook, Z. Feng, G. Gilliland, T. N. Bhat, H. Weissig, I. N. Shindyalov, P. E. Bourne, *Nucleic Acids Res.* **2000**, *28*, 235–242.

  

[4] C. X. Weichenberger, M. J. Sippl, *Bioinformatics* **2006**, *22*, 1397–1398.
[5] P. E. Hansen, *Magn. Reson. Chem.* **2000**, *38*, 1–10.
[6] T. Dziembowska, P. E. Hansen, Z. Rozwadowski, *Prog. Nucl. Magn. Reson. Spectrosc.* **2004**, *45*, 1–29.
[7] F. Hibbert, J. Emsley, *Adv. Phys. Org. Chem.* **1991**, *26*, 255–379.
[8] "Hydrogen Bond Isotope Effects Studied by NMR", H.-H. Limbach, G. S. Denisov, N. S. Golubev in *Isotope Effects in Chemistry and Biology* (Eds.: A. Kohen, H.-H. Limbach), CRC, Boca Raton, **2006**, pp. 193–230.
[9] A. C. LiWang, A. Bax, *J. Am. Chem. Soc.* **1996**, *118*, 12864–12865.
[10] M. Ottiger, A. Bax, *J. Am. Chem. Soc.* **1997**, *119*, 8070–8075.
[11] A. Meissner, J. Briand, O. W. Sørensen, *J. Biomol. NMR* **1998**, *12*, 339–343.
[12] A. Meissner, O. W. Sørensen, *J. Magn. Reson.* **1998**, *135*, 547–550.
[13] A. Liu, Y. Li, L. Yao, H. Yan, *J. Biomol. NMR* **2006**, *36*, 205–214.
[14] A. Liu, L. Yao, Y. Li, H. Yan, *J. Magn. Reson.* **2007**, *186*, 319–326.
[15] C. J. Jameson, *Bull. Magn. Reson.* **1981**, *3*, 3–29.
[16] E. Tüchsen, P. E. Hansen, *Int. J. Biol. Macromol.* **1991**, *13*, 2–8.
[17] J. G. Sośnicki, P. E. Hansen, *Tetrahedron Lett.* **2005**, *46*, 839–842.
[18] J. G. Sośnicki, M. Langaard, P. E. Hansen, *J. Org. Chem.* **2007**, *72*, 4108–4116.
[19] D. M. LeMaster, J. C. Laluppa, D. M. Kushlan, *J. Biomol. NMR* **1994**, *4*, 863–870.
[20] M. Ramanadham, S. K. Sikka, R. Chidamboram, *Acta Crystallogr. Sect. B: Struct. Crystallogr. Cryst. Chem.* **1972**, *28*, 3000–3005.
[21] J. J. Verbist, M. S. Lehman, K. T. F. , W. C. Hamilton, *Acta Crystallogr. Sect. B: Struct. Crystallogr. Cryst. Chem.* **1972**, *28*, 3006–3013.
[22] J. Herzfeld, J. E. Roberts, R. G. Griffin, *J. Chem. Phys.* **1987**, *86*, 597–602.
[23] K. Pervushin, R. Riek, G. Wider, K. Wüthrich, *Proc. Natl. Acad. Sci. USA* **1997**, *94*, 12366–12371.
[24] C. Griesinger, O. W. Sørensen, R. R. Ernst, *J. Chem. Phys.* **1986**, *85*, 6837–6852.
[25] J. Feeney, P. Partington, G. C. K. Roberts, *J. Magn. Reson.* **1974**, *13*, 268–274.
[26] G. E. Hawkes, E. W. Randall, W. E. Hull, D. Gattegno, F. Conti, *Biochemistry* **1978**, *17*, 3986–3992.
[27] M. Kainosho, T. Tsuji, *Biochemistry* **1982**, *21*, 6273–6279.
[28] E. Tüchsen, P. E. Hansen, *Biochemistry* **1988**, *27*, 8568–8576.
[29] P. E. Hansen, E. Tüchsen, *Acta Chem. Scand.* **1989**, *43*, 710–712.
[30] V. F. Bystrov, *Prog. Nucl. Magn. Reson. Spectrosc.* **1976**, *10*, 41–81.
[31] M. L. Cai, Y. Huang, G. M. Clore, *J. Am. Chem. Soc.* **2001**, *123*, 8642–8643.
[32] A. Liu, Z. Lu, J. Wang, L. Yao, Y. Li, H. Yan, *J. Am. Chem. Soc.* **2008**, *130*, 2428–2429.
[33] T.-P. Ko, J.-J. Lin, C.-Y. Hu, Y.-H. Hsu, A. H.-J. Wang, S.-H. Liaw, *J. Biol. Chem.* **2003**, *278*, 19111–19117.
[34] G. C. Ireton, M. E. Black, B. L. Stoddard, *Structure* **2003**, *11*, 961–972.
[35] J. Abildgaard, P. E. Hansen, A. E. Hansen, *J. Cell. Biochem.* **1995**, 68–68.
[36] C. X. Weichenberger, M. J. Sippl, *Nucleic Acids Res.* **2007**, *35*, W403–W406.
[37] V. A. Higman, J. Boyd, L. J. Smith, C. Redfield, *J. Biomol. NMR* **2004**, *30*, 327–346.
[38] I. W. Davis, A. Leaver-Fay, V. B. Chen, J. N. Block, G. J. Kapral, X. Wang, L. W. Murray, W. B. Arendall III, J. Snoeyink, J. S. Richardson, D. C. Richardson, *Nucleic Acids Res.* **2007**, *35*, W375–W383.
[39] L. Yao, S. Sklenak, H. Yan, R. I. Cukier, *J. Phys. Chem. B* **2005**, *109*, 7500–7510.
[40] D. A. Case, T. E. I. Cheatham, T. Darden, H. Gohlke, R. Luo, K. M. J. Merz, A. Onufriev, C. Simmerling, B. Wang, R. J. Woods, *J. Comput. Chem.* **2005**, *26*, 1668–1688.
[41] Y. Duan, C. Wu, S. Chowdhury, M. C. Lee, G. M. Xiong, W. Zhang, R. Yang, P. Cieplak, R. Luo, T. Lee, J. Caldwell, J. M. Wang, P. Kollman, *J. Comput. Chem.* **2003**, *24*, 1999–2012.
[42] L. Yao, Y. Li, Y. Wu, A. Liu, H. Yan, *Biochemistry* **2005**, *44*, 5940–5947.
[43] F. Delaglio, S. Grzesiek, G. W. Vuister, G. Zhu, J. Pfeifer, A. Bax, *J. Biomol. NMR* **1995**, *6*, 277–293.
[44] B. A. Johnson, R. A. Blevins, *J. Biomol. NMR* **1994**, *4*, 603–614.
[45] S. N. Loh, J. L. Markley, *Biochemistry* **1994**, *33*, 1029–1036.
[46] Y. Duan, C. Wu, S. Chowdhury, M. C. Lee, G. M. Xiong, W. Zhang, R. Yang, P. Cieplak, R. Luo, T. Lee, J. Caldwell, J. M. Wang, P. Kollman, *J. Comput. Chem.* **2003**, *24*, 1999–2012.
[47] H. J. C. Berendsen, J. P. M. Postma, W. F. Vangunsteren, A. Dinola, J. R. Haak, *J. Chem. Phys.* **1984**, *81*, 3684–3690.
[48] J. P. Ryckaert, G. Ciccotti, H. J. C. Berendsen, *J. Comput. Phys.* **1977**, *23*, 327–341.
[49] U. Essmann, L. Perera, M. L. Berkowitz, T. Darden, H. Lee, L. G. Pedersen, *J. Chem. Phys.* **1995**, *103*, 8577–8593.

Received: July 9, 2008
Published online on October 30, 2008

  